

# Molecular and Multimodal Retinal Imaging Findings in a Multicentric Portuguese Cohort of Stargardt Disease

## Achados Moleculares e de Imagiologia Multimodal numa Amostra Multicêntrica de Doentes Portugueses com Doença de Stargardt

 Sara Geada<sup>1</sup>,  Cristina Santos<sup>2</sup>,  Sara Vaz-Pereira<sup>3,4</sup>,  Ana Marta<sup>5,6</sup>,  Marta Correia<sup>7</sup>,  Keissy Sousa<sup>8</sup>,  
 Mário Soares<sup>1</sup>, Ana Luísa Carvalho<sup>9,10,12</sup>,  Jorge Saraiva<sup>9,11,12</sup>,  Joaquim Murta<sup>1,12,13</sup>,  Rufino Silva<sup>1,12,13</sup>,  
 Luísa Coutinho Santos<sup>2</sup>,  João Pedro Marques<sup>1,12,13</sup>

<sup>1</sup> Department of Ophthalmology, Centro Hospitalar e Universitário de Coimbra, EPE, Coimbra, Portugal

<sup>2</sup> Instituto de Oftalmologia Dr. Gama Pinto, Lisbon, Portugal

<sup>3</sup> Department of Ophthalmology, Centro Hospitalar Universitário de Lisboa Norte, EPE - Hospital de Santa Maria, Lisbon, Portugal

<sup>4</sup> Department of Ophthalmology, Faculdade de Medicina, Universidade de Lisboa, Lisbon, Portugal

<sup>5</sup> Department of Ophthalmology, Centro Hospitalar e Universitário do Porto, EPE, Porto, Portugal

<sup>6</sup> Instituto Ciências Biomédicas Abel Salazar (ICBAS), Porto, Portugal

<sup>7</sup> Department of Ophthalmology, Centro Hospitalar de Lisboa Ocidental, EPE, Lisbon, Portugal

<sup>8</sup> Department of Ophthalmology, Hospital de Braga, Braga, Portugal

<sup>9</sup> Medical Genetics Unit, Hospital Pediátrico, Centro Hospitalar e Universitário de Coimbra, EPE, Coimbra, Portugal

<sup>10</sup> University Clinic of Genetics, Faculty of Medicine, University of Coimbra, Coimbra, Portugal

<sup>11</sup> University Clinic of Pediatrics, Faculty of Medicine, University of Coimbra, Coimbra, Portugal

<sup>12</sup> Clinical Academic Center of Coimbra, Coimbra, Portugal

<sup>13</sup> University Clinic of Ophthalmology, Faculty of Medicine, University of Coimbra (FMUC), Coimbra, Portugal

Recebido/Received: 2021-10-15 | Aceite/Accepted: 2021-12-12 | Publicado/Published: 2022-03-31

© Author(s) (or their employer(s)) and *Oftalmologia* 2022. Re-use permitted under CC BY-NC. No commercial re-use.

© Autor (es) (ou seu (s) empregador (es)) e *Oftalmologia* 2022. Reutilização permitida de acordo com CC BY-NC. Nenhuma reutilização comercial.

DOI: <https://doi.org/10.48560/rspo.25968>

## ABSTRACT

**INTRODUCTION:** Our purpose was to describe the molecular and multimodal retinal imaging findings in a cohort of Portuguese patients with a clinical diagnosis of Stargardt Disease (STGD1).

**METHODS:** Multicenter, cross sectional cohort study of consecutive patients with a clinical diagnosis of STGD1, referred from six Portuguese centers. All patients underwent a complete ophthalmological examination complemented by color fundus photography (CFP), fundus autofluorescence (FAF), optical coherence tomography (SD-OCT) and, when available, OCT-angiography (OCTA). Proband with confirmed molecular diagnosis, defined as presenting biallelic mutations classified as pathogenic or likely pathogenic in accordance with the guidelines of the American College of Medical Genetics and Genomics, were divided into three groups according their genotype's severity.

**RESULTS:** The study included 122 eyes from 61 patients, 54 of which unrelated. Mean age of onset (AO) and mean disease duration were 16.64±12.87 and 20.04±15.21 years, respectively. Confirmed molecular diagnosis was obtained for 26/38 families with available genetic results (diagnostic yield of 68.42%), with the c.1804C>T (p.Arg602Trp) missense variant being the most prevalent (8/26). The less severe genotype group (Group C) was the most frequent (14/26), with

a mean AO slightly superior, not statistically significant, to the other groups (B and A). The most frequent CFP pattern was central atrophy with macular and/or peripheral flecks (56 eyes), followed by multiple extensive atrophic changes (n=40). On FAF, 21.05% of the eyes showed a homogeneous background with localized central hypoAF (pattern 1), with the remaining distributing equally through patterns 2 (heterogeneous background of hypo/hyperAF foci and localized central hypoAF) and 3 (multiple areas of hypoAF in a heterogeneous background). Worse visual acuity significantly correlated with advanced CFP and FAF patterns (both  $p<0.001$ ), reduced central macular thickness ( $p=0.017$ ), larger foveal avascular zone ( $p<0.001$ ), reduced density of the superficial ( $p<0.001$ ) and deep capillary plexuses ( $p=0.017$ ), and increased area of choriocapillaris atrophy ( $p=0.007$ ).

**CONCLUSION:** This study describes the phenotypic and genotypic spectrum of STGD1 in a multicenter Portuguese cohort, revealing a satisfactory detection rate of disease-causing genotypes. The qualitative and quantitative imaging features presented a strong correlation with visual acuity and disease progression and may represent important outcome measures in the evaluation of new therapeutic targets.

**KEYWORDS:** Genetic Testing; Genotype; Phenotype; Retinal Dystrophies; Stargardt Disease.

## RESUMO

**INTRODUÇÃO:** O nosso objetivo foi caracterizar os achados moleculares e de imagiologia multimodal numa população portuguesa com doença de Stargardt (STGD1).

**MÉTODOS:** Estudo transversal, multicêntrico que incluiu doentes consecutivos com diagnóstico clínico de STGD1, provenientes de seis centros nacionais. Todos os doentes foram submetidos a um exame oftalmológico completo complementado por imagiologia multimodal - retinografia, autofluorescência do fundo (FAF), tomografia de coerência ótica (SD-OCT) e, quando disponível, angiografia por OCT (OCTA). Indivíduos com confirmação molecular, definida pela presença de mutações bialélicas classe IV ou V, foram divididos em 3 grupos de acordo com a gravidade do respetivo genótipo.

**RESULTADOS:** Foram incluídos 122 olhos de 61 doentes, 54 dos quais sem relação de parentesco. A idade média de início (AO) e a duração média da doença foram  $16,64\pm 12,87$  e  $20,04\pm 15,21$  anos, respetivamente. O diagnóstico molecular foi obtido para 26/38 famílias com estudo genético disponível (rendimento diagnóstico 68,42%), sendo a variante *missense* c.1804C>T (p.Arg602Trp) a mais prevalente (8/26). O grupo de genótipo menos grave (Grupo C) foi o mais frequente (14/26), com uma média de AO ligeiramente superior aos grupos A e B, embora não estatisticamente significativa. Na retinografia, o padrão mais frequente foi o de atrofia central com manchas amareladas maculares e/ou periféricas (56 olhos). Na FAF, 21,05% dos olhos apresentaram hypoAF central num fundo homogéneo (padrão 1), com os restantes distribuindo-se equitativamente pelos padrões 2 (focos de hypo/hiperAF e hypoAF central distribuídos por um fundo heterogéneo) e 3 (áreas múltiplas de hypoAF num fundo heterogéneo). Uma pior acuidade visual correlacionou-se com padrões avançados na retinografia e FAF ( $p<0,001$  para ambos), espessura macular central reduzida ( $p=0,017$ ), maior zona avascular da fóvea ( $p<0,001$ ), menor densidade vascular do plexos capilares superficial ( $p<0,001$ ) e profundo ( $p=0,017$ ) e maior área de atrofia coriocapilar ( $p=0,007$ ).

**CONCLUSÃO:** Este estudo descreve o espectro fenotípico e genotípico de uma coorte portuguesa multicêntrica com STGD1. As características qualitativas e quantitativas dos exames de imagem analisados apresentaram forte correlação com a acuidade visual e progressão da doença, podendo representar importantes meios de análise de resultados na avaliação de novos alvos terapêuticos.

**PALAVRAS-CHAVE:** Distrofias da Retina; Doença de Stargardt; Estudo Genético; Genótipo; Fenótipo.

## INTRODUCTION

Stargardt disease (STGD1, OMIM: 248200) is the most frequent macular juvenile dystrophy, with an estimated prevalence of 1:8 000 to 1:10 000.<sup>1-5</sup> It is caused by biallelic mutations in the adenosine triphosphate (ATP)-binding cassette A4 gene (*ABCA4*), which encodes a transmembrane protein involved in active transport of retinoids from photoreceptors to retinal pigment epithelium (RPE). Failure of this transport results in accumulation of cytotoxic lipofuscin fluorophores, namely A2E, in the RPE cells, leading to their dysfunction and death, with subsequent photoreceptor (PR) cell loss.<sup>6,7</sup> This explains two of the three hallmarks of the disease on fundoscopic examination: macular atrophy due to RPE and PR loss, which can expand beyond the posterior pole at late disease stage, and the yellowish white flecks that result from localized accumulation of RPE lipofuscin. The third fundoscopic finding that completes the diagnostic triad of STGD1 corresponds to peripapillary sparing of the above-mentioned retinal changes.<sup>1,6,7</sup>

Classically, patients present with bilateral central vision loss, secondary to macular atrophy, usually becoming apparent at early adolescence/young adulthood and evolving with gradual vision loss over disease progression.<sup>1,2,5,7</sup> However, both age of onset and the disease course vary extensively, and genotype-phenotype correlations have been established, with worse genotypes resulting in earlier onset and more rapid progression.<sup>1,3,5,7,8</sup>

STGD1 is inherited following an autosomal recessive pattern,<sup>1-7</sup> with a carrier frequency for potentially pathogenic *ABCA4* alleles of 1:20.<sup>3,7</sup> To date, > 1200 disease-causing variants have been reported,<sup>5,6</sup> with the majority consisting of missense mutations.<sup>5</sup> Grouping of these variants in severity categories according to their presumed functional effect has been proposed, varying from deleterious (stop-gained or frameshift insertion/deletion (indel)) to mild effect (missense or in-frame indel) in *ABCA4* activity.<sup>1-3,7</sup>

Visual function and disease progression have not only been correlated with genotype, but also with structural features, through extensive evaluation using multimodal retinal imaging comprising fundus autofluorescence (FAF), optical coherence tomography (OCT) and OCT-angiography (OCTA).<sup>1,2,4-6,8-13</sup> Typical findings on FAF include hyperautofluorescent (hyperAF) foci corresponding to the yellowish-white flecks, and hypoautofluorescent (hypoAF) areas at the level of RPE atrophy.<sup>1,4,6,9-12</sup> The hallmark on OCT is the general thinning in the central retina.<sup>4,10</sup> Regarding OCTA, central choriocapillaris atrophy, larger foveal avascular zone and reduced density of retinal capillary plexus have been reported in association with later stages in the disease course.<sup>4,10,13</sup>

The aim of this study was to characterize the molecular and multimodal retinal imaging findings in a large cohort of clinically diagnosed STGD1 Portuguese patients from six centers. Additionally, genotype-phenotype and structural-functional correlations were evaluated.

## MATERIAL AND METHODS

### STUDY DESIGN AND PATIENT SELECTION

We conducted a multicenter, cross sectional cohort study including 122 eyes from 61 consecutive patients diagnosed with STGD1 in the following Portuguese centers: Centro Hospitalar e Universitário de Coimbra (CHUC), Instituto de Oftalmologia Dr. Gama Pinto (IOGP), Centro Hospitalar e Universitário de Lisboa Norte (CHULN), Centro Hospitalar e Universitário do Porto (CHUP), Centro Hospitalar de Lisboa Ocidental (CHLO) and Hospital de Braga (HB). Sample distribution across these centers is shown in Fig. 1.

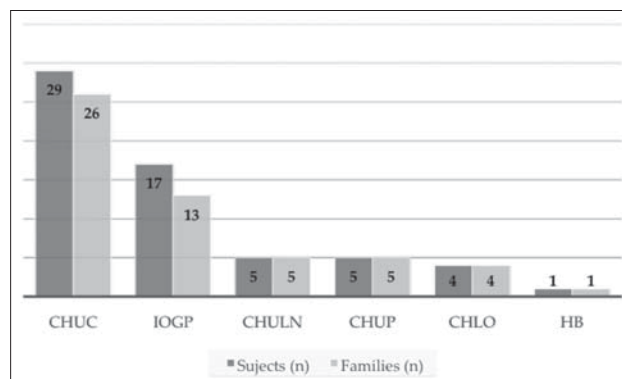


Figure 1. Sample distribution across the six Portuguese centers which contributed to the study.

CHUC – Centro Hospitalar e Universitário de Coimbra; IOGP – Instituto de Oftalmologia Dr. Gama Pinto; CHULN – Centro Hospitalar e Universitário de Lisboa Norte; CHUP – Centro Hospitalar e Universitário do Porto; CHLO – Centro Hospitalar de Lisboa Ocidental; HB – Hospital de Braga

The study was approved by the local Ethics Committees and followed the tenets of the Declaration of Helsinki for biomedical research. Written informed consent was obtained for every included subject.

Inclusion criteria consisted in a clinical diagnosis of STGD1 ± genetic testing. The clinical diagnosis was based on patient history of central vision loss as the main symptom, along with family history compatible with autosomal recessive inheritance, and typical changes on dilated fundus examination (macular RPE atrophy, yellowish-white flecks and peripapillary sparing). Patients with significant media opacities, unstable fixation, or those with any possibly confounding vitreoretinal disease were excluded.

### GENETIC TESTING

For probands with available molecular results at the time of data collection (n=47), the genetic testing consisted in either eye-gene enriched panel-based next-generation sequencing (NGS) or whole exome sequencing (WES), complemented by multiplex ligation-dependent probe amplification (MLPA) when deemed necessary. Peripheral blood samples were collected according to the manufacturer's specifications for whole-blood

DNA extraction. Whenever possible, segregation analysis was performed in family members, whose samples were analyzed by Sanger sequencing to search for the variants detected in their respecting probands. Genetic counselling provided by a medical geneticist was granted to all subjects.

The diagnostic yield was calculated from the number of families with confirmed disease causing genotypes, consisting in the presence of two mutating alleles whose variants were classified as pathogenic (class V) or likely pathogenic (class IV) in accordance with the guidelines of the American College of Medical Genetics and Genomics.<sup>14,15</sup>

Patients with confirmed molecular diagnosis were further divided into 3 groups according to the genotype classification proposed by Fujinami *et al*<sup>1</sup>: Group A included patients harboring 2 predictive deleterious (nonsense, splice-site or frameshift) variants; Group B included subjects presenting one deleterious and one missense or in-frame indel variant; Group C included patients presenting biallelic missense/in-frame indels variants.

## CLINICAL/DEMOGRAPHIC FEATURES

A detailed medical history was obtained for every patient and included natural history, age at diagnosis, age of onset of symptoms, disease duration, family history and the presence of consanguinity in the family.

The age of onset was defined as the age at which the visual loss was noted by the patient or his carriers, in case of childhood onset.

The disease duration was calculated as the difference between the subject's age at the date this study was conducted and the age of onset.

## OPHTHALMIC EXAMINATION, MULTIMODAL IMAGING AND GRADING

All patients underwent a comprehensive ophthalmologic examination including: (1) best-corrected visual acuity (BCVA), converted to equivalent ETDRS letters (for counting finger (CF) and hand movement (HM) was attributed the value 0 ETDRS); (2) dilated slit-lamp anterior segment and fundus biomicroscopy; (3) multimodal imaging comprising color fundus photography (CFP), blue-light FAF imaging, spectral-domain OCT (SD-OCT), and OCTA when available.

CFP and FAF aspects were divided into four and three groups, respectively, according to the classification proposed by Fujinami *et al*<sup>1</sup>: CFP grade 1: normal fundus; CFP grade 2: macular and/or peripheral flecks without central atrophy; CFP grade 3a: central atrophy without flecks; CFP grade 3b: central atrophy with macular and/or peripheral flecks; CFP grade 3c: paracentral atrophy with macular and/or peripheral flecks, without central atrophy; CFP grade 4: multiple extensive atrophic changes of the RPE, extending beyond the vascular arcades. Regarding AF: grade 1: localized low AF signal at the fovea surrounded by a homogeneous background, with/without perifoveal foci of high or low AF signal; grade 2: localized low AF signal at the macula surrounded by a heterogeneous background, and widespread foci

of high or low AF signal extending anterior to the vascular arcades; grade 3: multiple areas of low AF signal at the posterior pole with a heterogeneous background, with/without foci of high or low AF signal. The presence of peripapillary sparing on FAF examination was also noted.

On SD-OCT, photoreceptor ellipsoid zone (EZ) preservation in central retina was evaluated and divided into the three categories described by Liu, Fujinami and associates<sup>16</sup>: Category 1: preserved EZ in the fovea; Category 2: loss of EZ in the fovea; Category 3: extensive loss of EZ. The central macular thickness (CMT), corresponding to the distance (expressed in micrometer,  $\mu\text{m}$ ) between the inner limiting membrane to the inner border of the RPE, was also measured using SD-OCT.<sup>1</sup>

On OCTA, 6x6-mm high-definition (400x400) scans were obtained for measuring the following parameters: (1) macular vascular density of superficial (SMVD) and deep capillary plexus (DMVD); (2) central choriocapillaris atrophy (CCA); (3) foveal avascular zone (FAZ). The parameters (2) and (3) were manually outlined through the free-hand selection tool on the OCTA equipment, and their dimension was expressed as squared millimeters ( $\text{mm}^2$ ).<sup>4,17</sup>

## STATISTICAL ANALYSIS

Statistical analysis was performed using the SPSS program (SPSS Statistics, version 15 for Windows, SPSS Inc., IBM, Somers, NY). Descriptive analysis was performed for all study variables. Continuous variables were recorded as mean and standard deviation (SD) values with minimum and maximum when appropriate, whereas categorical variables were recorded as absolute and relative frequencies. Normality was evaluated through the Kolmogorov-Smirnov test for each variable. Comparison between continuous variables was performed using the T-Student test, when parametric, and Mann-Whitney U test, when non-parametric distribution was obtained. Categorical variables were tested for association using chi-square test. Pearson's and Spearman's bivariate correlation tests were used to studying correlations. Regression analysis was performed using genotype grouping and adjusting for disease duration to predict BCVA (using ETDRS letters). *P* values less than 0.05 were considered statistically significant.

## RESULTS

### DEMOGRAPHIC AND CLINICAL DATA

A total of 61 patients (122 eyes), 54 of which unrelated, were enrolled in the study, coming from 12 of the 18 Portuguese Continental Districts. Demographic and clinical data of the study population are summarized in Table 1. Almost half (25/61) presented a positive family history, and 9 were from consanguineous families. The mean age of onset (AO) was 16.64±12.87 years, range 3-52, with more than half (33/61) reporting an AO before 18 years, while only 12 initiated symptoms after 30 years. The mean age at diagnosis (AD) was 27.21±16.01, with a maximum time between AO and AD of 38 years in one patient.

The disease duration ranged from 1 to 52 years, with an average of 20.04±15.21 years.

**Table 1. Demographic and clinical data of the study population.**

<b>Eyes/Patients (n)</b>	122/61
<b>Female patients (n; %)</b>	33; 54.10
<b>Age</b>	
Mean (years)	41.28±17.29
Range (years)	9-78
Pediatric patients (age <18 years) (n)	4
<b>Families (n)</b>	
<b>Mean age at diagnosis (years)</b>	27.21±16.01
<b>Age of onset</b>	
Mean age of onset (years)	16.64±12.87
Onset before 18 years (n; %)	33; 54.10
Onset after 30 years (n; %)	12; 19.67
<b>Disease Duration</b>	
Mean disease duration (years)	20.04±15.21
Disease duration < 10 years (n;%)	18; 11.00
Disease duration > 20 years (n;%)	28; 45.90
<b>Mean visual acuity (ETDRS letters)</b>	
Right eye	30.00
Left eye	30.95

AF – autofluorescence; OCT – optical coherence tomography; EZ – photoreceptor ellipsoid zone.

The mean visual acuity was 30.00 and 30.95 ETDRS letters in the right and left eye, respectively (ranging from 0 to 75 letters in both eyes). Worse visual acuity significantly correlated with a longer disease duration ( $p<0.001$ ).

## MULTIMODAL RETINAL IMAGING

Frequency of CFP, FAF and OCT patterns across the study population is represented in Table 2, as well as the summarized data collected for continuous variables evaluated on SD-OCT (CMT) and OCT-A (macular vascular density of superficial and deep capillary plexus, central choriocapillaris atrophy and foveal avascular zone).

Fifty-six eyes were classified into grade 3b on CFP, the most frequently observed pattern (45.90%), followed by grade 4 which was attributed to 31.15% (40/122) of the eyes. Thirteen eyes (7 patients) presented typical flecks but no central atrophy (grade 2). None of the eyes showed normal fundus appearance (pattern 1), and only two corresponded to grade 3c.

In eyes with available FAF imaging (n=114), grade 1 was the least common (24 eyes), while grades 2 and 3 were equally observed in the remaining eyes. Peripapillary sparing on AF was present in 75.44% (86/114) of the eyes.

Examples of different CFP and FAF grades, observed in some of our probands, are represented in Fig. 2 and 3, respectively.

**Table 2. Retinal imaging findings and their statistical analysis in the study population.**

Retinal imaging	
Color Fundus Photography	n (%)
Grade 1: Normal	0 (0)
Grade 2: Macular and/or peripheral flecks without central atrophy	13 (10.66)
Grade 3	69 (56.56)
Grade 3a: Central atrophy without flecks	11 (9.02)
Grade 3b: Central atrophy with macular and/or peripheral flecks	56 (45.90)
Grade 3c: Paracentral atrophy with macular and/or peripheral flecks without central atrophy	2 (1.64)
Grade 4: Multiple extensive atrophic changes of the RPE, extending beyond vascular arcades	40 (32.79)
Fundus Autofluorescence	n (%)
Grade 1: Localized low AF signal at the fovea surrounded by a homogeneous background with/without perifoveal foci of high or low signal	24 (21.05)
Grade 2: Localized low AF signal at the macula surrounded by a heterogeneous background and widespread foci of high or low AF signal extending anterior to the vascular arcade	45 (39.47)
Grade 3: Multiple areas of low AF signal at posterior pole with a heterogeneous background and/or foci of high or low signal	45 (39.47)
Optical coherence tomography	n (%)
Category 1: Preserved EZ in the fovea	7(6.14)
Category 2: Loss of EZ in the fovea	35 (30.70)
Category 3: Extensive loss of EZ	72 (63.16)
OCT/OCTA quantitative features	Mean±SD
Central macular thickness (µm)	120.24±48.60
Macular vascular density of superficial capillary plexus (%)	45.16±5.38
Macular vascular density of deep capillary plexus (%)	42.82±4.38
Central choriocapillaris atrophy (mm <sup>2</sup> )	12.86±12.54
Foveal avascular zone (mm <sup>2</sup> )	1.10±0.82

AF – autofluorescence; EZ – photoreceptor ellipsoid zone; OCT – optical coherence tomography; OCTA – OCT – angiography; SD – standard deviation;

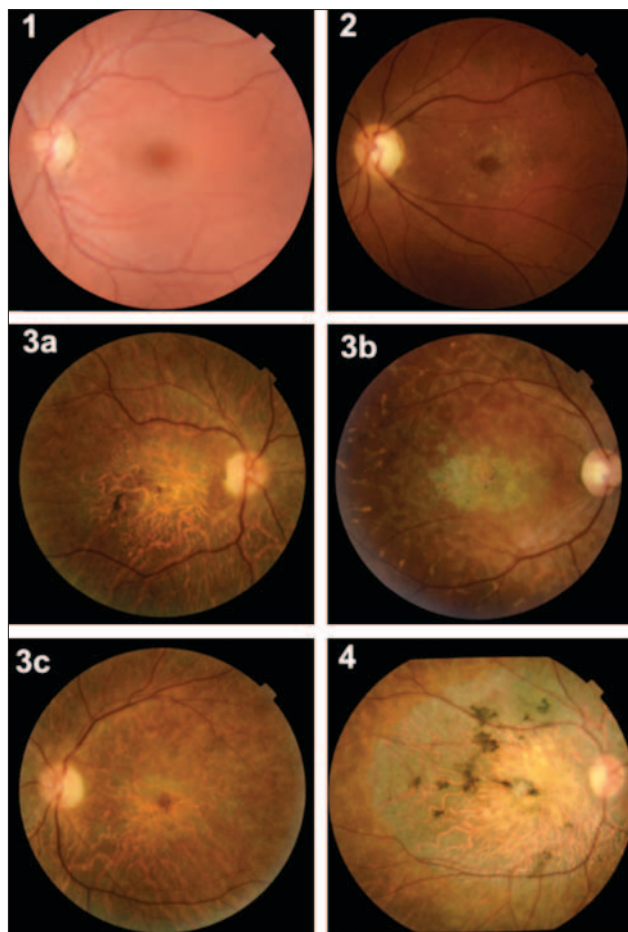


**Figure 2.** Examples of the color fundus photography grades. (1) normal fundus; (2) macular and/or peripheral flecks without central atrophy; (3a) central atrophy without flecks; (3b) central atrophy with macular and/or peripheral flecks; (3c) paracentral atrophy with macular and/or peripheral flecks, without central atrophy; (4) multiple extensive atrophic changes of the RPE, extending beyond the vascular arcades

Regarding SD-OCT (n=114), extensive loss of the EZ (category 3) was the most frequent finding (63.16%; 72 eyes). Only 7 eyes (4 patients) showed foveal EZ preservation (category 1). In this subgroup, the AO was  $26.00 \pm 12.69$  (range 5-37) and the disease duration was >10 years except for one

proband (6 years). All patients excluding one had genetically solved disease (Genotype 3); in the molecular unsolved subject, for whom no clinically significant variants were found, an asymmetry between eyes was noted (only one eye showed foveal EZ sparing), and the age of onset was 5 years (against the remaining patients in that group, who all reported first symptoms around age of 30 years).

Intereye symmetry was present in all patients on blue-light FAF. On the other hand, 3 patients showed different sub-patterns inside grade 3 between OD and OS on CFP and 2 patients had intereye asymmetry on SD-OCT.

There were significant differences regarding multimodal imaging findings and disease duration, with more advanced grades on CFP, FAF and OCT correlating with longer disease duration ( $p < 0.001$  for all three imaging methods). The same was true for BCVA, with more severe vision loss significantly associated to worse CFP ( $p < 0.001$ ), FAF ( $p < 0.001$ ), and OCT ( $p < 0.001$ ) grades.

Mean CMT was  $120.24 \pm 48.60$   $\mu\text{m}$ . Thinner measurements were significantly associated with worse BCVA ( $p = 0.017$ ) but did not show correlation with disease progression ( $p = 0.210$ ).

For the subset of eyes with OCTA data (n=34), all the evaluated parameters (SMVD, DMVD, FAZ and CCA) showed a significant correlation with BCVA, with less ETDRS letters corresponding to reduced SMVD ( $p < 0.001$ ) and DMVD ( $p = 0.017$ ), larger FAZ ( $p < 0.001$ ), and increased CCA ( $p = 0.007$ ). However, only CCA proved to significantly correlate with disease duration ( $p = 0.026$ ).

### ABCA4 VARIANTS

Confirmed molecular diagnosis was obtained for 26/38 families with available genetic results, for a diagnostic yield of 68.42%. In other 4 families, the probands had a disease-causing variant with one variant of uncertain significance in trans, and, hence, it was not possible to genetically confirm the diagnosis. For the remaining 8 families, no clinically significant variants were found in the probands with available genetic results.

In total, 25 pathogenic/likely pathogenic variants were identified, distributed across 56 alleles (26 families with pathogenic/likely pathogenic variants in the two alleles, and 4 families with confirmed disease causing variant in only one allele). The characterization of these variants is presented in Table 3. The majority of mutations were classi-

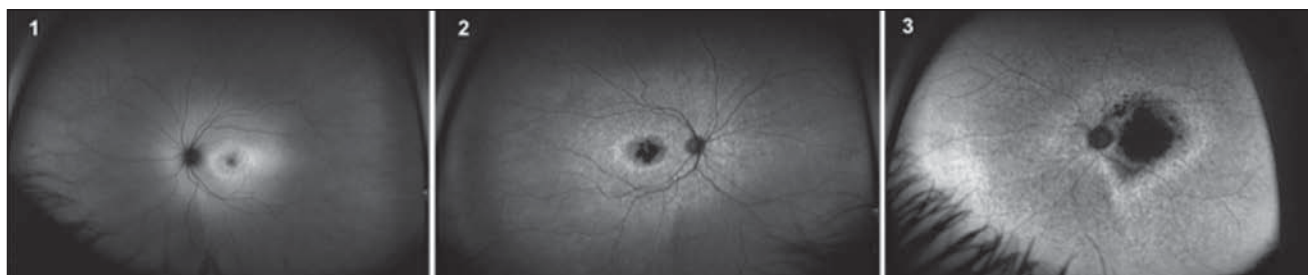


**Figure 3.** Examples of the fundus autofluorescence grades observed in patients of our cohort. (1) localized low AF signal at the fovea surrounded by a homogeneous background, with/without perifoveal foci of high or low AF signal; (2) localized low AF signal at the macula surrounded by a heterogeneous background, and widespread foci of high or low AF signal extending anterior to the vascular arcades; (3) multiple areas of low AF signal at the posterior pole with a heterogeneous background, with/without foci of high or low AF signal.

**Table 3.** ABCA4 variants found in the 38 Portuguese families with available genetic results.

Nucleotide	Protein	Functional effect	Clinical significance	Families (n)	Alleles (n)	Zygoty
c.1804C>T	p.Arg602Trp	Missense	Pathogenic	8	9	hz, CHz
c.3210_3211dup	p.Ser1071Cysfs*14	Frameshift	Pathogenic	4	5	hz, CHz
c.5882 G>A	p.Gly1961Glu	Missense	Pathogenic	4	4	CHz
c.4720G>T	p.Glu1574*	Stopgain	Pathogenic	4	4	CHz
c.32T>C	p.Leu11Pro	Missense	Likely pathogenic	3	4	hz, CHz
c.4139C>T	p.Pro1380Leu	Missense	Likely pathogenic	3	3	CHz
c.286A>G	p.Asn96Asp	Missense	Likely pathogenic	2	3	hz, CHz
c3113C>T	p.Ala1038Val	Missense	Likely pathogenic	2	2	CHz
c.5327C>T	p.Pro1776Leu	Missense	Pathogenic	2	2	CHz
c.5044_5058del	p.Val1682_Val1686del	In-frame deletion	Pathogenic	2*	2*	CHz*
c.464C>T	p.?	Splice site	Pathogenic	1	6	hz
c.634C>T	p.Arg212Cys	Missense	Likely pathogenic	1	2	hz
c.5461-10T>C	p.?	Splice site	Pathogenic	1	2	CHz
c.4926C>G	p.Ser1642Arg	Missense	Likely pathogenic	1*	1*	CHz*
c.6089G>A	p.Arg2030Gln	Missense	Likely pathogenic	1	1	CHz
c.6079C>T	p.Leu2027Phe	Missense	Likely pathogenic	1	1	CHz
c.6104T>C	p.Leu2035Pro	Missense	Likely pathogenic	1	1	CHz
c.6088C>T	p.Arg2030Ter	Stopgain	Pathogenic	1	1	CHz
c.4328G>A	p.Arg1443His	Missense	Pathogenic	1	1	CHz
c.2588G>C	p.Gly863Ala	Missense	Likely pathogenic	1	1	CHz
c.3386G>T	p.Arg1129Leu	Missense	Likely pathogenic	1	1	CHz
c.6320G>A	p.(Arg2107His)	Missense	Likely pathogenic	1	1	CHz
c.834del	p.Asp279Ilefs*21	Frameshift deletion	Likely pathogenic	1	1	CHz
c.(658_766)_ (768+199_769-1)del	p.?	Deletion	Likely pathogenic	1	1	CHz
c.5196+1137G>A	p.?	Intronic	Likely pathogenic	1	1	CHz

hz – homozygosity; CHz – compound heterozygosity

\*Variants found in complex alleles

fied as missense, representing 76.00% (19/25) of all the variants. The most frequent mutations found in our cohort were c.1804C>T (p.Arg602Trp) (9/56 alleles), c.464C>T (p.?) (6/56 alleles), c.3210\_3211dup (p.Ser1071Cysfs\*14) (5/56), c.5882 G>A (p.Gly1961Glu) (4/56), c.4720G>T (p.Glu1574\*) (4/56) and c.32T>C (p.Leu11Pro) (4/56). One proband presented a complex allele, with the variant c.5044\_5058del (p.Val1682\_Val1686del) and c.4926C>G (p.Ser1642Arg) in cis and the c.1804C>T(p.Arg602Trp) in trans.

## GENOTYPE GROUPS

For probands with genetically solved SGGT1 (32 subjects, 26 families), the genotype group C (biallelic missense/in-frame variants) was the most frequent, with 16/30 patients (14/26 families, 53.84%). Only 5 patients (3 families, 11.53%) presented biallelic deleterious variants (Group A). The remaining 11 subjects (9 families, 34.62%) were included in group B, harboring one deleterious and one missense/in-frame variant.

Group A presented a mean age of onset of 8.8±1.33 years, inferior to that calculated for group B (13.45±7.82 years), which in turn was inferior to Group C (15.94±12.13 years). However, these differences were not statistically significant ( $p=0.270$ ).

A multiple linear regression was conducted to predict BCVA based on genotype and disease duration. A significant model was found ( $F(2,53)=13.25$ ,  $p<0.001$ ), with an  $R^2$  of 0.333. Even though disease duration was a significant predictor of lower BCVA ( $p<0.001$ ), genotype was not ( $p=0.303$ ).

## DISCUSSION

By combining data from 6 national Ophthalmology Departments, this study reports molecular and multimodal imaging findings from a large Portuguese cohort with STGD1.

Deep phenotyping by means of multimodal retinal imaging has shown to be of crucial value, since it provides information regarding disease natural history and prognosis.<sup>1,8,9,11,12,16,18</sup> In our study, almost 80% of the eyes presented

macular atrophy associated with macular/peripheral flecks (grade 3b), or multiple extensive atrophic changes of the RPE extending beyond vascular arcades (grade 4). CFP patterns significantly correlated with disease duration. This is in accordance with other studies that evaluated adult populations with STGD1.<sup>2,1</sup> Absence of central macular atrophy was present in only about 10% of the eyes.<sup>6</sup> Foveal sparing is a rare finding especially in cohorts with an earlier age of onset,<sup>1,8,16</sup> which generally is related with a worse phenotype.<sup>1,7,8,16</sup> It has been associated with less severe disease and later disease onset.<sup>1,6</sup> The mean AO in our cohort (16.64 years) was inferior to that reported by other authors (approximately 19 years),<sup>2,6,19</sup> and more than a half of the study population reported onset of symptoms before 18 years old. The earlier AO in our study could probably explain the small percentage of eyes presenting foveal sparing, which may also be supported by the later mean AO in the subgroup of patients with foveal EZ preservation on SD-OCT. Regarding FAF patterns, patterns 2 and 3 were observed with the same frequency in our cohort, while pattern 1 was the least frequent (~25% eyes). Progression across FAF grades over time has been reported,<sup>1,6,12</sup> which explains the positive correlation between FAF patterns and disease duration that we describe. Disease duration also demonstrated a positive correlation with the extension of EZ loss on SD-OCT. Interestingly, this was not the case for CMT. Finally, OCTA has been increasingly used to analyze the retinal and choroidal vasculatures in all types of retinal diseases, including IRDs.<sup>4,13</sup> Our findings suggest a complex vascular impairment and confirms that important changes occur in the different retinal vascular plexuses and in the choriocapillaris. We have shown that reduced SMVD and DMVD, increased FAZ and larger CCA atrophy in these patients are significantly associated with worse BCVA. Additionally, a larger CCA area significantly correlated with longer disease duration.

It is important to note that FAF and SD-OCT imaging was not possible to classify in 4 patients (8 eyes) due to insufficient image quality and/or lack of collaboration. Only one center provided OCTA, explaining the small percentage of patients with available results. These aspects constitute an important limitation of our study regarding deep phenotype characterization.

By using clinically-oriented genetic testing based on targeted NGS, this study revealed a total of 26 pathogenic/likely pathogenic variants in the *ABCA4* gene in a group of 26 Portuguese families, with the great majority (76.00%) being functionally classified as missense variants. This is in accordance with previous reports.<sup>2,3,7,20</sup>

The variant c.1804C>T (p.Arg602Trp) was the most prevalent in our cohort, observed in 8/26 families (30.77%). It was reported as the fourth more common mutation in a large Spanish cohort,<sup>3</sup> responding for 5% of the families studied, and has been described as a frequent mutation in Caucasians.<sup>3,21</sup> as well as in the South African population.<sup>22</sup> Interestingly, this variant was also the most prevalent variant observed in a Taiwan cohort.<sup>18</sup> It is reported to be a severe missense variant associated with rapid progression.<sup>18</sup> However, due to the small number of probands with available genetic results and to the cross-sectional design of our study,

it was not possible to ascertain these genotype-phenotype correlations.

On the other hand, the most prevalent mutation in the above mentioned Spanish study, that englobed 506 families with biallelic *ABCA4* pathogenic variants, was the p.(Arg1129Leu),<sup>3</sup> which seems to have a high prevalence in Hispanic populations, since it was also one of the most frequent mutations verified in a Argentinean cohort.<sup>2</sup> In our study, however, it was identified in only one family.

The mutation c.5882 G>A (p.Gly1961Glu) is the most common among STGD1 patients from different ethnic backgrounds, with an allele frequency in European population of ~0.4%<sup>7</sup> and with a variable frequency of 6.5%-21% in diverse STGD cohorts.<sup>2</sup> In a large international cohort, the ProgStar study report 8, conducted by Fujinami *et al*,<sup>19</sup> p.(Gly1961Glu) was the most prevalent mutation, with a frequency of 15%. In the present study, it was observed in 4/26 families (15.38%).

In one proband, the most frequently reported intronic variant in *ABCA4*, the c.5196+1137G>A, was found in association with one deleterious variant in trans. However, this patient presented a relatively mild phenotype, with a later age of onset (27 years) and relatively preserved BCVA (50 ETDRS letters OU). This is in keeping with previous reports, that consider that intronic variant of intermediate effect, producing a significant milder phenotype when in trans with null mutation (when compared with two null alleles).<sup>23</sup>

Regarding genotype groups, we included 11.53% of families in Group A, 34.62% in Group B and 53.84% in Group C. These results are in accordance with the findings presented by Fujinami *et al* in the ProgStar study report 8, with approximately half of probands belonging to Group C (49.8%).<sup>19</sup> In a Chinese adult cohort,<sup>16</sup> with an earlier mean AO (10.0 years) and in a pediatric cohort<sup>1</sup> a higher proportion of families was included in Group A (around 20%) and the Genotype B was the most frequent (approximately 45%). These findings support the hypothesis that the distribution of deleterious variants in a STGD1 cohort depends on the age of onset, with worse genotypes resulting in an earlier AO and worse phenotypes.<sup>1,3,7,16</sup>

In previous studies, a statically significant difference was noted between genotype groups and mean age of onset.<sup>1,3</sup> Also, differences in BCVA have been shown to exist between genotype groups, with group A showing the worse BCVA for the same disease duration and age.<sup>16</sup> Although an increase in mean AO from group A to group C was observed in our cohort, this was not statistically significant. Additionally, when considering disease duration, BCVA did not differ across genotype groups. This may be explained by three possible bias, which represent important limitations of our study: (1) the small number of families with available genetic testing results may not be representative of the population, thus limiting the statistical power to establish those correlations; (2) assigning functional effect to a mutation was not always straightforward, especially for missense alleles and some variants in splice sites – this has been appointed in other studies as a general limitation of the segregation trough genotype groups, since the functional consequences not always correlate exactly with resulting disease phenotypes and progression<sup>7</sup>; and (3) the exact AO cannot be easily

determined, as many patients (particularly children) may be unaware of their visual impairment, and this turns especially difficult when trying to provide it in retrospective recall.

Besides the above mentioned, other significant limitations should be noted. First, a significant part of our cohort has not been genetically tested (14/52 families), which does not allow us to exclude potential phenocopies. These account for 10%-15% of all cases of *ABCA4*-associated phenotypes.<sup>7</sup> Second, 4 patients harbored a variant of uncertain significance for whom family segregation analysis was not enough to reclassify the variant's pathogenicity. Accordingly, these patients could not be included in a genotype group. Third, the cross-sectional design does not provide information regarding disease natural history and progression.

## CONCLUSION

To the best of our knowledge, this is the largest study to describe the phenotypic and genotypic spectrum of STGD1 in a multicentric Portuguese cohort, revealing a satisfactory detection rate of disease-causing genotypes. Deep phenotyping using multimodal retinal imaging (CFP, FAF, OCT and OCTA) was shown to be of clinical utility in the evaluation of these patients. Imaging biomarkers evaluated here presented a strong correlation with BCVA and disease progression. These qualitative and quantitative imaging features may represent important outcome measures in the efficacy evaluation of new therapeutic targets. Due to the reduced number of probands with available genetic results, our study was not powerful enough to establish genotype-phenotype correlations. Longitudinal studies englobing larger samples with genetically confirmed diagnosis are warranted to assess genotype-phenotype correlations and predict disease progression, based not only on molecular aspects but also on deep phenotyping by means of multimodal retinal imaging.

## PRESENTATIONS AND AWARDS

This study was awarded "Best Scientific Poster Presentation" at "Reunião do Grupo Português de Retina e Vítreo", October 15-16th 2021, Coimbra, Portugal.

## CONTRIBUTORSHIP STATEMENT / DECLARAÇÃO DE CONTRIBUIÇÃO:

SG: Colheita e análise de dados; elaboração do manuscrito (escrita e formatação).

CS, SV-P, AM, MC, KS e ALS.: Colheita de dados; revisão do manuscrito.

MS: Colheita de dados.

JS, JM, RS e LC-S: Seleção da amostra; revisão do manuscrito.

JPM: Seleção da amostra; , elaboração e revisão do manuscrito.

## RESPONSABILIDADES ÉTICAS

**Conflitos de Interesse:** Os autores declaram a inexistência de conflitos de interesse na realização do presente trabalho.

**Fontes de Financiamento:** Não existiram fontes externas de financiamento para a realização deste artigo.

**Confidencialidade dos Dados:** Os autores declaram ter seguido os protocolos da sua instituição acerca da publicação dos dados de doentes.

**Proteção de Pessoas e Animais:** Os autores declaram que os procedimentos seguidos estavam de acordo com os regulamentos estabelecidos pelos responsáveis da Comissão de Investigação Clínica e Ética e de acordo com a Declaração de Helsinquia revista em 2013 e da Associação Médica Mundial.

**Proveniência e Revisão por Pares:** Não comissionado; revisão externa por pares.

## ETHICAL DISCLOSURES

**Conflicts of Interest:** The authors have no conflicts of interest to declare.

**Financing Support:** This work has not received any contribution, grant or scholarship

**Confidentiality of Data:** The authors declare that they have followed the protocols of their work center on the publication of data from patients.

**Protection of Human and Animal Subjects:** The authors declare that the procedures followed were in accordance with the regulations of the relevant clinical research ethics committee and with those of the Code of Ethics of the World Medical Association (Declaration of Helsinki as revised in 2013).

**Provenance and Peer Review:** Not commissioned; externally peer reviewed.

## REFERENCES

1. Fujinami K, Zernant J, Chana RK, Wright GA, Tsunoda K, Ozawa Y, et al. Clinical and molecular characteristics of childhood-onset Stargardt disease. *Ophthalmology*. 2015;122:326-34. doi: 10.1016/j.ophtha.2014.08.012.
2. Mena MD, Moresco AA, Vidal SH, Aguilar-Cortes D, Obregon MG, Fandiño AC, et al. Clinical and Genetic Spectrum of Stargardt Disease in Argentinean Patients. *Front. Genet.* 2021;12:646058. doi: 10.3389/fgene.2021.646058
3. Del Pozo-Valero M, Riveiro-Alvarez R, Blanco-Kelly F, Aguirre-Lamban J, Martin-Merida I, Iancu IF, et al. Genotype-Phenotype Correlations in a Spanish Cohort of 506 Families With Biallelic *ABCA4* Pathogenic Variants. *Am J Ophthalmol.* 2020;219:195-204. doi: 10.1016/j.ajo.2020.06.027..
4. Battaglia Parodi M, Cicinelli MV, Rabiolo A, Pierro L, Bolognesi G, Bandello F. Vascular abnormalities in patients with Stargardt disease assessed with optical coherence tomography angiography. *Br J Ophthalmol.* 2017;101:780-5. doi: 10.1136/bjophthalmol-2016-308869.
5. Rahman N, Georgiou M, Khan KN, Michaelides M. Macular dystrophies: clinical and imaging features, molecular genetics

- and therapeutic options. *Br J Ophthalmol.* 2020;104:451–460.
6. Fujinami K, Lois N, Mukherjee R, McBain VA, Tsunoda K, Tsubota K, et al. A longitudinal study of Stargardt disease: quantitative assessment of fundus autofluorescence, progression, and genotype correlations. *Invest Ophthalmol Vis Sci.* 2013;54:8181–90. doi: 10.1167/iovs.13-12104.
  7. Cremers FPM, Lee W, Collin RWJ, Allikmets R. Clinical spectrum, genetic complexity and therapeutic approaches for retinal disease caused by ABCA4 mutations. *Prog Retin Eye Res.* 2020;79:100861. doi: 10.1016/j.preteyeres.2020.100861.
  8. Holtan JP, Aukrust I, Jansson RW, Berland S, Bruland O, Gjerde BL, et al. Clinical features and molecular genetics of patients with ABCA4-retinal dystrophies. *Acta Ophthalmol.* 2021;99:e733–e746. doi: 10.1111/aos.14679
  9. Klufas MA, Tsui I, Sadda SR, Hosseini H, Schwartz SD. Ultrawidefield autofluorescence in ABCA4 Stargardt disease. *Retina.* 2018;38:403–15. doi: 10.1097/IAE.0000000000001567.
  10. Arrigo A, Grazioli A, Romano F, Aragona E, Marchese A, Bordato A, et al. Multimodal evaluation of central and peripheral alterations in Stargardt disease: a pilot study. *Br J Ophthalmol.* 2020;104:1234–8. doi:10.1136/bjophthalmol-2019-315148
  11. Müller PL, Gliem M, McGuinness M, Birtel J, Holz FG, Issa PC. Quantitative Fundus Autofluorescence in ABCA4 -related retinopathy – Functional Relevance and Genotype- Phenotype Correlation. *Am J Ophthalmol.* 2021;222:340–50. doi:10.1016/j.ajo.2020.08.042 .
  12. Georgiou M, Kane T, Tanna P, Bouzia Z, Singh N, Kalitzeos A, et al. Prospective Cohort Study of Childhood-Onset Stargardt Disease: Fundus Autofluorescence Imaging, Progression, Comparison with Adult-Onset Disease, and Disease Symmetry. *Am J Ophthalmol.* 2020;211:159–75. doi: 10.1016/j.ajo.2019.11.008.
  13. Jauregui R, Cho A, Lee W, Zernant J, Allikmets R, Sparrow JR, et al. Progressive choriocapillaris impairment in ABCA4 maculopathy is secondary to retinal pigment epithelium atrophy. *Invest Ophthalmol Vis Sci.* 2020;61:13. doi:10.1167/iovs.61.4.13
  14. Richards S, Aziz N, Bale S, Bick D, Das S, Gastier-Foster J, et al. Standards and guidelines for the interpretation of sequence variants: a joint consensus recommendation of the American College of Medical Genetics and Genomics and the Association for Molecular Pathology. *Genet Med.* 2015;17:405–24.
  15. Cornelis SS, Bax NM, Zernant J, Allikmets R, Fritsche LG, den Dunnen JT, et al. In silico functional meta-analysis of 5,962 ABCA4 variants in 3,928 retinal dystrophy cases. *Hum Mutat.* 2017;38:400–8.
  16. Liu X, Meng X, Yang L, Long Y, Fujinami-Yokokawa Y, Ren J, et al. Clinical and genetic characteristics of Stargardt disease in a large Western China cohort: Report 1. *Am J Med Genet C Semin Med Genet.* 2020;1–14. doi:10.1002/ajmg.c.31838.
  17. Samara WA, Say EA, Khoo CT, Higgins TP, Magrath G, Ferenczy S, et al. Correlation of foveal avascular zone size with foveal morphology in normal eyes using optical coherence tomography angiography. *Retina.* 2015;35:2188–95.
  18. Sung YC, Yang CH, Yang CM. Genotypes Predispose Phenotypes—Clinical Features and Genetic Spectrum of ABCA4-Associated Retinal Dystrophies. *Genes.* 2020;11:1421. doi:10.3390/genes11121421
  19. Fujinami K, Strauss RW, Chiang JPW, Audo IS, Bernstein PS, Birch DG, et al. Detailed genetic characteristics of an international large cohort of patients with Stargardt disease: ProgStar study report 8. *Br J Ophthalmol.* 2018;103:390–7. doi: 10.1136/bjophthalmol-2018-312064.
  20. Garces FA, Scortecchi JF, Molday RS. Functional Characterization of ABCA4 Missense Variants Linked to Stargardt Macular Degeneration. *Int J Mol Sci.* 2021;22:185. doi:10.3390/ijms22010185.
  21. Maia-Lopes S, Aguirre-Lamban J, Castelo-Branco M, Riveiro-Alvarez R, Ayuso C, Silva ED. ABCA4 mutations in Portuguese Stargardt patients: identification of new mutations and their phenotypic analysis. *Mol Vis.* 2009;15:584–91.
  22. Roberts L, Nossek CA, Greenberg LJ, Ramesar RS. Stargardt macular dystrophy: Common ABCA4 mutations in South Africa—Establishment of a rapid genetic test and relating risk to patients. *Molecular Vision.* 2012;18:280–9.
  23. Khan M, Arno G, Fakin A, Parfitt DA, Dhooze PPA, Albert S, et al. Detailed Phenotyping and Therapeutic Strategies for Intronic ABCA4 Variants in Stargardt Disease. *Mol Ther Nucleic Acids.* 2020;21:412–27. doi: 10.1016/j.omtn.2020.06.007.



**Corresponding Author/  
Autor Correspondente:**

**Sara Geada**

Centro Hospitalar e Universitário de Coimbra (CHUC)  
Praceta Prof. Mota Pinto  
3000-075 Coimbra, Portugal  
sarageadabatista@gmail.com



ORCID: 0000-0002-6851-6201